IPI Letters

ISSN 2976 – 730X
IPI Letters (1): 84 - 91, 2023
https://doi.org/10.59973/ipil.43

Received: 2023-12-21
Accepted: 2023-12-25
Published: 2023-12-27

Editorial Article

BORIS – Micromagnetic, Spin Transport and Multiscale Atomistic Software for Modelling Magnetic Information Storage

Serban Lepadatu [1*]

[1] Jeremiah Horrocks Institute for Mathematics, Physics and Astronomy, University of Central Lancashire, Preston PR1 2HE, U.K.

*Corresponding author (Email: SLepadatu@uclan.ac.uk)

Abstract – A brief review of BORIS is given here, together with a review of recent works using this software, including applications to modelling magnetic hard-disk-drive read heads, ultrafast magnetization processes, computation of thermodynamic equilibrium states using Monte Carlo algorithms, and modelling skyrmions as information carriers. BORIS is a state-of-the-art multi-physics and multi-scale research software designed to solve three-dimensional magnetization dynamics problems, coupled with a self-consistent charge and spin transport solver, heat flow solver with temperature-dependent material parameters, and elastodynamics solver including thermoelastic and magnetoelastic/magnetostriction effects, in arbitrary multi-layered structures and shapes. Both micromagnetic and atomistic models are implemented, also allowing multi-scale modelling where computational spaces may be configured with multiple simultaneous micromagnetic and atomistic discretization regions. The software allows multi-GPU computations on any number of GPUs in parallel, in order to accelerate simulations and allow for larger problem sizes compared to single-GPU computations – this is the first magnetization dynamics software to allow multi-GPU computations, enabling large problems encompassing billions of cells to be simulated with unprecedented performance.

Keywords – BORIS; Atomistic modelling of magnetic information storage; Skyrmions; Multi-GPU computations;

1. Introduction

BORIS is a multi-physics research software oriented towards modelling magnetization processes [1]. Micromagnetic and atomistic discretizations are allowed, and it is specifically designed as a multi-mesh and multi-scale software. Magnetization dynamics are computed using the Landau-Lifshitz-Gilbert (LLG) equation [2], or the Landau-Lifshitz-Bloch (LLB) equation [3], either of which may be augmented by thermal fluctuations (stochastic versions) [4,5], Zhang-Li spin transfer torques (STT) [6], interfacial STT (ISTT) [7,8], spin-orbit torques (SOT) due to the spin-Hall effect (SHE) [9], Slonczewski spin torques [10], or spin torques computed self-consistently using a spin transport solver. The spin transport solver self-consistently calculates charge currents, spin currents, and spin accumulations in multi-layer structures [11]. In addition to obtaining spin torques self-consistently several effects may be computed, including anisotropic magneto-resistance (AMR), current perpendicular to plane giant magneto-resistance (CPP-GMR), SHE and inverse SHE (ISHE) [12], spin pumping [13], charge pumping and topological Hall effect [14,15]. Recently tunneling magneto-resistance (TMR) has also been included in the spin transport solver [16]. A heat solver is also available, allowing calculation of heat flow in response to ambient conditions as well as sources and sinks. An important source of heat is due to Joule heating from a current density calculated using the transport solver. This allows inclusion of temperature-dependent effects in the magnetization dynamics, including AMR-generated magnonic spin-Seebeck effect [17]. Another heat source is due to ultrafast laser pulses, and a two-temperature model (2TM) is included to allow simulations of ultrafast demagnetization and recovery processes [18]. Additionally, a two-sublattice model is implemented, allowing simulations of antiferromagnetic and ferrimagnetic materials, fully integrated within the multi-mesh computational paradigm, allowing for example simulations with exchange bias.
The computational meshes can be sized and discretized independently. One of the most difficult interactions to

compute across several independent computational meshes is the magnetostatic interaction. A newly developed method, termed multi-layered convolution [19], allows computation of demagnetizing fields for multiple meshes with arbitrary thicknesses, arbitrary relative positioning and spacings, without impacting on the computational performance. Other long-range interactions include the Oersted field, which is computed from the current density obtained using the transport solver, as well as stray field computation from a number of fixed magnetic dipoles. Individual magnetic mesh modules include magneto-crystalline anisotropy (MCA), either uniaxial or cubic, direct exchange interaction, Dzyaloshinsky-Moriya interaction (DMI) [20,21], either bulk or interfacial, surface exchange coupling [22], topographical surface and edge roughness [23].

The software has a modular structure and is open-source [24]. A graphical user interface is provided for interactive display of simulation data, with user control enabled through a graphical console allowing intuitive and interactive control of simulations, shown in Figure 1. The software may also be controlled using Python scripts which communicate with BORIS through network sockets, thus allowing either local or remote user control. Additionally, embedded Python scripts may also be executed, where BORIS itself acts as the Python interpreter, thus allowing complex simulations flows to be configured by the user.

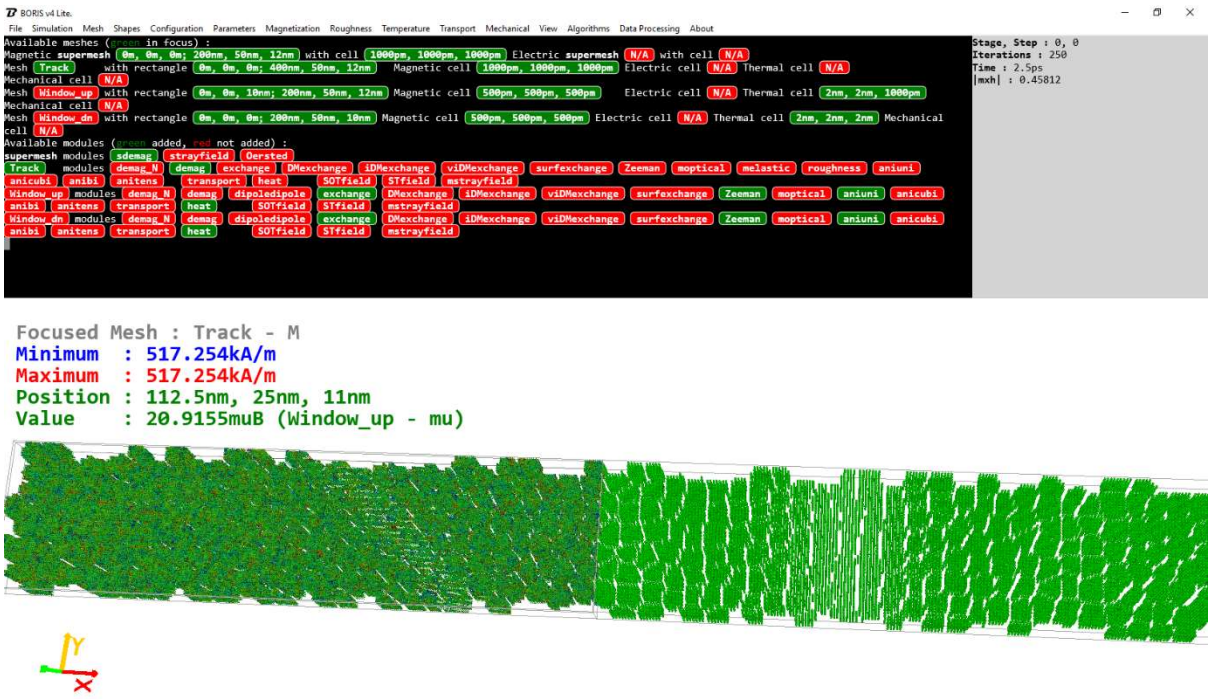

Figure 1. BORIS graphical interface, including an interactive computational space display, a graphical console and output data box for monitoring. Whilst simulation workflows are best configured using Python scripts, full manual control is possible through the console and menu.

The software has been programmed mainly in C++17 and CUDA C, as well as Python. Supported operating systems include Windows, and Linux-based distributions. All computational routines can be executed on central processing units (CPU), as well as graphical processing units (GPU) using the CUDA framework [25].

In the latest version all GPU computations have been upgraded to allow multiple GPUs to be used simultaneously in order to reduce computation time, but also to allow for a larger simulation size than is possible on a single GPU [26], where it was shown that using a single workstation with 4 GPUs, atomistic spin dynamics simulations with up to 1 billion spins, and atomistic Monte Carlo simulations with up to 2 billion spins are possible, with a near-ideal performance scaling.

2. Magnetic Hard Disk-Drive Read-Heads

A three-dimensional self-consistent spin transport model was developed in Ref. [16], which includes both tunneling transport, leading to TMR, as well as metallic transport, leading to giant magneto-resistance. The model is able to include not only TMR, but also spin torques arising across a tunnel barrier. Metallic pin-hole defects may be included in the tunnel barrier, and it was shown that even a single pinhole defect can significantly degrade the performance of tunnel junctions and magnetic read-heads below the 40 nm node. The model was further applied to the analysis of a realistic hard-disk-drive (HDD) TMR read-head, in order to compute the signal-to-noise ratio (SNR), and the effect of bias on it – a generic stack of an HDD reader is shown in Figure 2. The free layer (FL) is biased by side shields, approximated by permanent magnets. A synthetic antiferromagnet (SAF) is comprised of the reference layer (RL), exchange coupled to the pinned layer (PL) via Ruderman–Kittel–Kasuya–Yosida (RKKY) interactions in a 0.8nm thick Ru spacer layer. The PL is stabilized by exchange coupling to an underlying antiferromagnetic (AFM) layer.

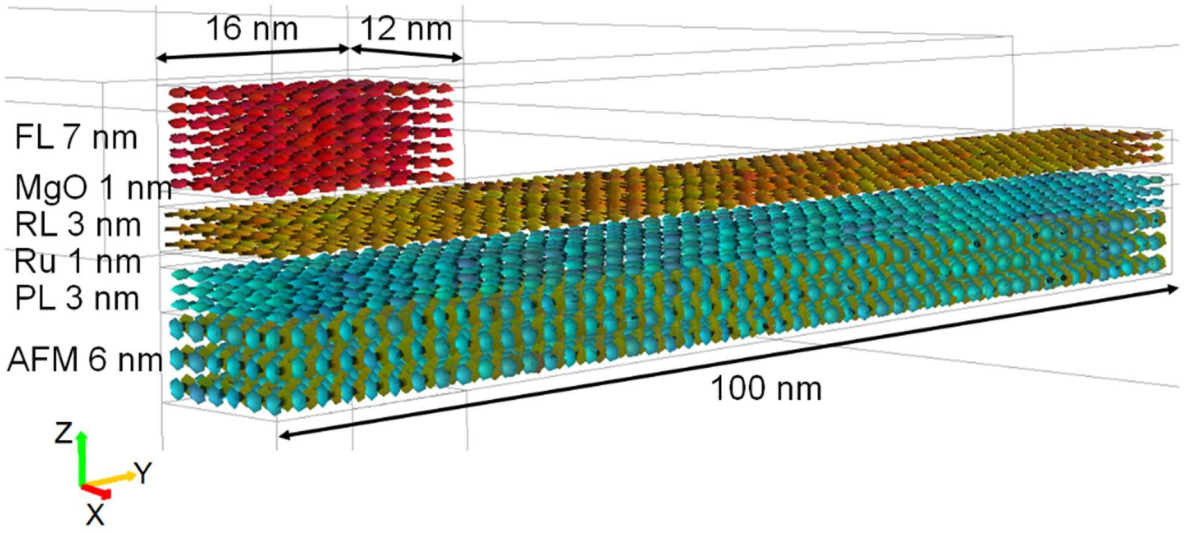

Figure 2. A model of a realistic magnetic read head, containing of a synthetic antiferromagnetic stack (PL/Ru/RL), with the pinned layer (PL) fixed by the antiferromagnetic layer (AFM). The free layer (FL) is highly sensitive to external fields, and any rotation with respect to the reference layer (RL) results in large changes in resistance due to TMR through the MgO barrier. Image adapted from Ref. [16].

Spin torques in magnetic read-heads can induce instabilities which results in increased magnetic noise. This was investigated in Ref. [16] by applying a potential across the stack in Figure 2. Spin-torques are then computed self-consistently, whose effect on magnetization thermal fluctuations is to amplify them with increasing potential strength. It was shown that above a certain threshold potential the SNR abruptly decreases, thus setting a limit on the maximum reading potential possible.

In addition to modelling read heads, magnetic information writing processes may also be modelled using BORIS. In a recent work a multi-scale model was developed for the purpose of simulating heat-assisted magnetic recording (HAMR) processes in granular magnetic tracks – details to be included in an upcoming publication. The multi-scale model includes an arbitrarily long magnetic track with a granular structure, discretized using a micromagnetic formalism, however only a small portion of the track is evolved dynamically using a moving simulation window. The simulation window contains atomistic discretization, either with a simple cubic lattice structure, or with a realistic crystal structure such as face-centred-cubic or hexagonal-close-packed. This allows inclusion of thermal effects from a circular laser spot with Gaussian profile, where the temperature can exceed the Curie temperature. Together with a polarity-controlled external magnetic field profile, granular bits may be written at a controlled simulation window velocity within the larger magnetic track. The simulation window can consist entirely of atomistic discretization, but also of a combination of micromagnetic and atomistic regions, e.g. a micromagnetic/atomistic/micromagnetic arrangement centred on the laser spot. These regions are exchange coupled, and the magnetostatic field is fully included between them, as well as the contribution from the larger magnetic track. This allows an efficient HAMR modelling process, whilst allowing high temperature regions to be computed accurately in the atomistic spin dynamics formalism.

3. Ultrafast Magnetic Processes

An ultrafast laser pulse can cause rapid demagnetization, followed by magnetization recovery [27]. On the ultrafast timescale (femtosecond timescale) it is known that conduction and lattice electrons respond on very different timescales, which is modelled through different specific heat capacities in a two-temperature model. An example of such a simulation was given in Ref. [26]. The effect of the laser pulse is shown in Figure 3: the electron bath temperature increases rapidly on a fs timescale, with temperatures exceeding the Curie temperature. After the laser pulse the electron bath temperature decreases rapidly as it equilibrates with the slower changing lattice temperature. This results in an initial rapid demagnetization, followed by a slower recovery process as the temperature decreases. A uniform external field of 1 MA/m is applied into the plane, which results in magnetization switching on a longer timescale as seen in Figure 3. It should be noted this process is similar to the mechanism used for HAMR as discussed in the previous section. What is important about this example, is the computations were done using 4 GPUs in parallel, which allowed an unprecedented simulation dimension, comprising ~0.5 billion atomistic spins, simulated in a practical time-frame (~12 h for each simulated nanosecond).

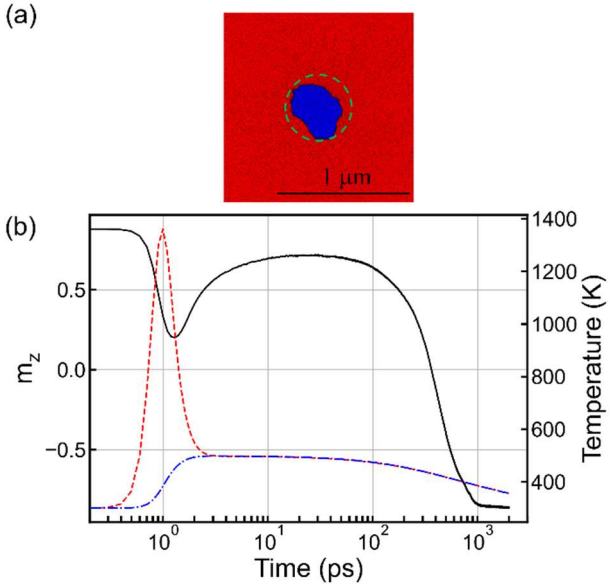

Figure 3. Ultrafast demagnetization and magnetization reversal under a uniform external field, computed using atomistic spin dynamics coupled to the 2-temperature heat equation, in a 16 nm thick FePt film. (a) The m_z component simulation snapshot, with red positive and blue negative, at 400 ps. The laser spot size is indicated with the dashed green circle. (b) The m_z component of normalized magnetization as a function of time for a problem with ~0.5 billion spins is plotted, in response to an ultrafast laser pulse with Gaussian temporal and spatial profiles. The electron bath and lattice temperatures are shown using the dashed red line and dash-dot blue line respectively. Image adapted from Ref. [26].

Another example of the effect an ultrafast laser pulse can have on magnetization processes is the work in Ref. [28]. Here, the possibility of creating a single Néel skyrmion after ultrafast demagnetization was investigated, both in antiferromagnets and ferromagnets. It was shown that whilst magnetization switching can be induced deterministically, the creation of a number of Néel skyrmions is described by a Poisson distribution. Due to the high degree of disorder after ultrafast demagnetization, the nucleation of Néel skyrmions is accompanied by the nucleation of domain wall skyrmions, which results in a self-annihilation collapse. Domain wall skyrmions [29] are a 360º degree rotation of the in-plane magnetization components transverse to an out-of-plane Néel domain wall – this is depicted in Figure 4 – with an integer topological charge. During magnetization recovery processes such chiral kinks are found at the domain wall boundary of nucleated skyrmions. As discussed in Ref. [28], whilst such topological objects are highly unstable, they do play an important role in mediating interactions between nucleated skyrmions, resulting in repulsive interactions for objects with same topological charge, as well as annihilations between objects with opposite topological charges.

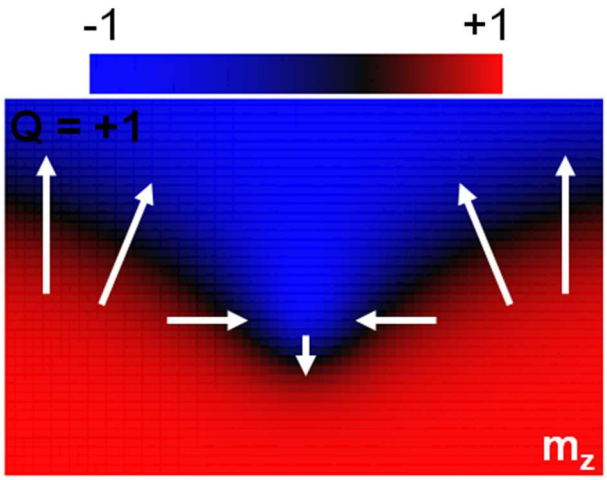

Figure 4. DW skyrmion with topological charge Q = +1, showing the magnetization z component, with overlaid sketch of the in-plane components of magnetization. Image adapted from Ref. [28].

4. Monte Carlo Algorithms

Whilst computation of magnetization dynamics processes is important, equally important is the requirement to compute states of thermodynamic equilibrium. An obvious example here is computation of finite-temperature hysteresis loops. Whilst such modelling can be done using the usual magnetization dynamics equation (e.g. stochastic LLG or stochastic LLB), the dynamical approach to relaxation is very inefficient. Instead, Monte Carlo methods are far more efficient. In Ref. [30] a new Monte Carlo algorithm was introduced, specifically for modelling at the micromagnetic length scale (MMC), where a variable magnetization length was used based on the LLB equation. A number of applications were discussed, where in addition to finite-temperature hysteresis loop modelling, chiral magnetic thin films, granular magnetic media, and artificial spin ices were also modelled. The algorithm can be executed on single GPUs, as well as multiple GPUs, where a red-black checkerboard decomposition scheme is used, as previously introduced for modelling atomistic spin systems in BORIS [31]. Importantly, the long-range magnetostatic interaction is also included in the algorithm, introduced such that data race conditions do not occur, whilst still allowing accurate computations of the effect of magnetostatic fields on thermodynamic equilibrium states.

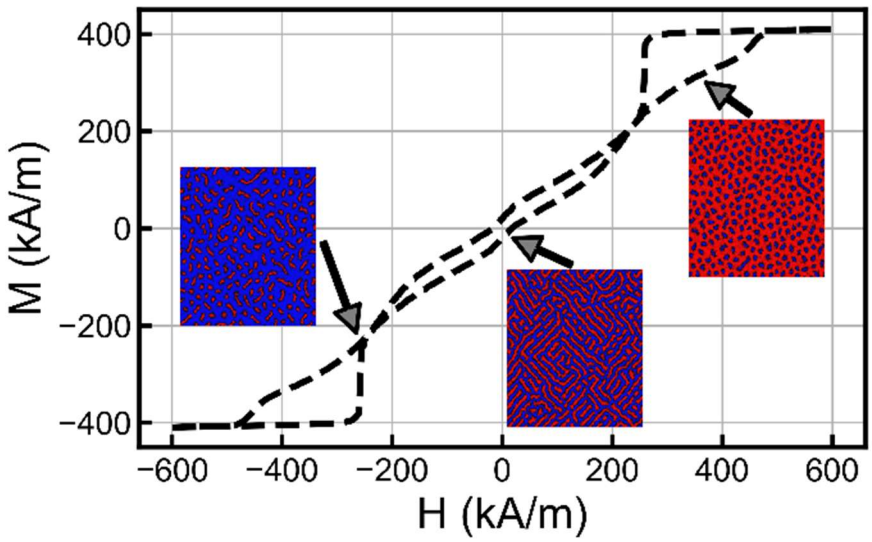

Figure 5. Hysteresis loop in a 2 nm thin Co film with interfacial DMI and perpendicular anisotropy, computed at 350 K using the micromagnetic Monte Carlo algorithm. The insets show the perpendicular magnetization component at the indicated points on the increasing field sweep, with blue denoting magnetization into the plane, and red out of the plane. Image adapted from Ref. [30].

An example computation using the MMC algorithm is shown in Figure 5, as discussed in Ref. [30]. Here a hysteresis loop is computed at 350 K in a 2 nm thin Co film with interfacial DMI interaction and perpendicular anisotropy. A

labyrinth domain structure is observed at zero field, resulting in a heared hysteresis loop. Inspecting the increasing field sweep, the labyrinth domain structure is suddenly formed at a negative field, nucleated through thermal activation, as indicated in the inset to Figure 5. As the field strength is increased the labyrinth domain structure is gradually reduced, eventually forming a small number of skyrmions. Further increasing the field results in thermal annihilation of skyrmions, leading to saturation. Modelling results are similar to experimental results in Ref. [32].

Another Monte Carlo computation is included in Ref. [33], exemplifying how information states gradually vanish due to self-erasure. Over time this reduces the information entropy of the system according to the second law of information dynamics. Using the concept of information entropy, in analogy to the second law of thermodynamics, it was shown it must remain constant or decrease over time, in contrast with physical entropy which increases over time.

5. Skyrmions as Information Carriers

In Ref. [34] it was shown that magnetic skyrmions, in metallic multilayers such as Co/Pt, can be controllably moved on surfaces simply using a focused laser beam – this is exemplified in Figure 6. Temperature gradients generated at the focused laser spot directly result in skyrmion motion due to magnetic parameter temperature dependences.

However, another contribution which can be even more important, and has not been considered so far, is due to thermoelastic lattice expansion, resulting in a local strain-induced magnetic anisotropy gradient. This method of all-optically generated skyrmion displacement allows full control of motion over two-dimensional magnetic surfaces, with a possible method of MEMS-VCSEL on-chip integration.

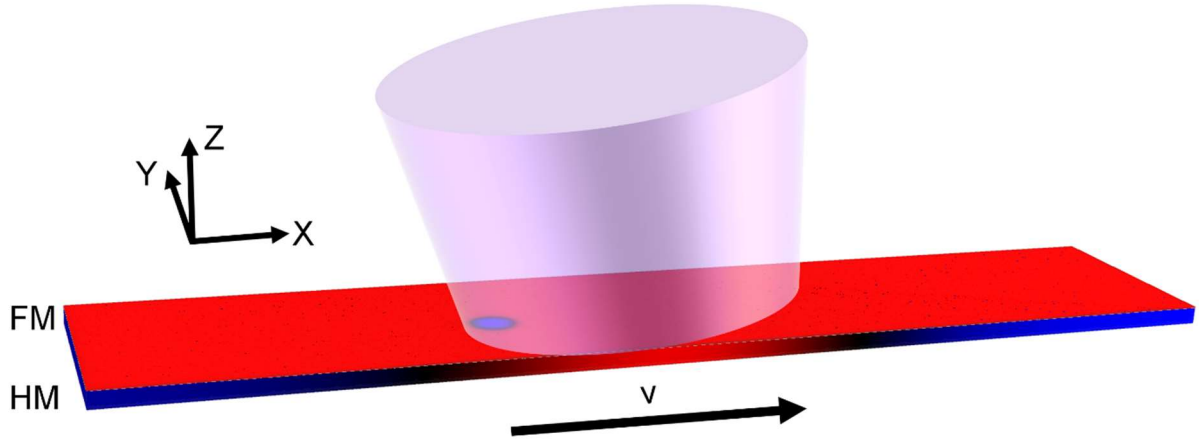

Figure 6. Skyrmion motion generated by scanning a focused laser beam, due to magneto-thermo-elastic coupling in a magnetic track. The skyrmion is moved using a focused laser beam (1 mW absorbed power) and with a set velocity along the track (v = 20 m/s). In the FM layer, red indicates magnetization out of the plane, and blue into the plane. Image adapted from Ref. [34].

The computations in Ref. [34] are performed in BORIS using three coupled dynamics solvers – namely for magnetization (LLG equation), temperature (heat flow equation), and strain (elastodynamics equations). The LLG equation is coupled to the temperature as the magnetization length is temperature dependent, and also to the strain through the magneto-elastic effect. The elastodynamics equation also includes the effect of magnetostriction, and is also coupled to the heat equation through the thermo-elastic effect. Such coupling of different solvers within a multi-physics package allows complex simulations to be performed.

Whilst in Ref. [34] it was shown skyrmions may be manipulated using a focused laser beam, the most common method of moving skyrmions involves the use of electrical currents as shown in a joint experimental and computational work in Ref. [35]. Here the motion of a large number of skyrmions in multi-layered Pt/Co/Ir structures was investigated, by coupling the magnetization dynamics equation to the self-consistent spin transport solver.

In addition to the usual SOT and bulk STT contributions, it was demonstrated an addition important spin torque arises, namely the interfacial STT (ISTT). The ISTT is generated due to diffusive vertical spin currents in multilayers – the spin accumulation generated at magnetization gradients (here at skyrmions) results in spin currents flowing away from the ferromagnetic layers into the adjacent metallic layers.

Due to conservation of total angular momentum a strong spin torque is generated as exemplified in Figure 7. The ISTT has important implications for the current-induced motion of magnetic skyrmions, resolving discrepancies between experiments and modelling with SOT alone. In particular, the small skyrmion Hall angles and velocities observed in experiments cannot be reproduced using the SOT alone with realistic material parameters, whilst inclusion of ISTT obtains results in good agreement with experimental observations [35].

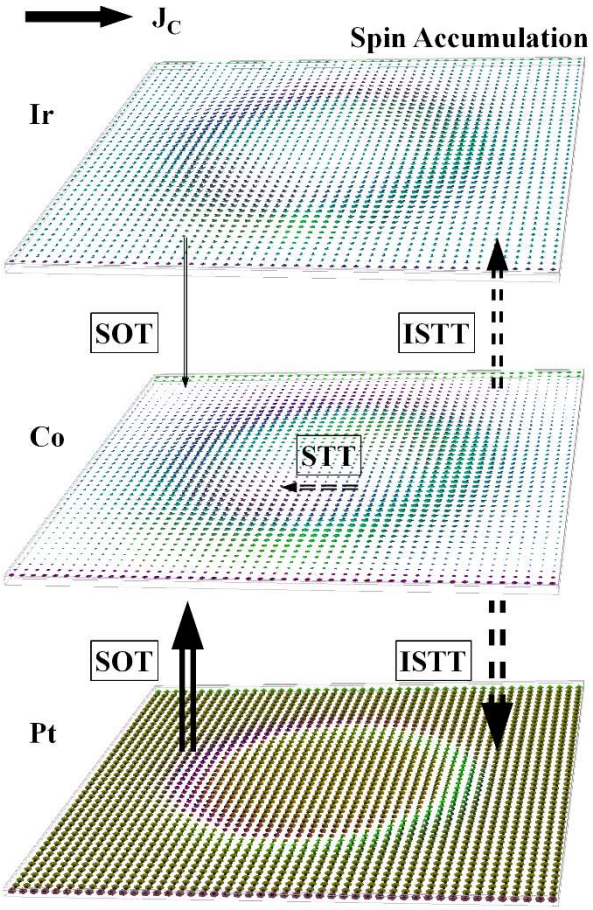

Figure 7. Diagrammatic representation of the origins of different spin torques in a Pt/Co/Ir multilayer. The SHE gives rises to vertical spin currents (indicated by solid arrows) flowing from Pt (and to a much smaller extent Ir) into Co, resulting in SOT. Spin accumulation at the skyrmion in Co gives rise to diffusive vertical spin currents (dashed arrows), flowing from Co into Pt and Ir, resulting in ISTT. Spin accumulation at the skyrmion in Co also gives rise to in-plane spin currents (small dashed arrow), resulting in the much weaker bulk STT. Image reproduced from Ref. [35].

6. Conclusion

Here a review of BORIS was given, which is a relatively new comprehensive computational magnetism research software. A multi-mesh modelling paradigm is used, which allows complex simulations with multiple independently discretized computational meshes and materials. Both micromagnetic and atomistic discretizations are allowed within the same computational space. In addition to simple cubic lattices for atomistic models, recently realistic crystal structures have also been implemented, namely body-centred-cubic, face-centred-cubic, hexagonal-close-packed, as well as arbitrary user-defined unit cells, with exchange interactions extending to any number of neighbours. Moreover, the magnetization dynamics solvers may be coupled to the heat flow equation, both one and two-temperature models, elastodynamics equations, and a self-consistent spin transport solver. This allows complex simulations of multi-material structures, including ferromagnetic, antiferromagnetic, ferrimagnetic, as well as non-magnetic and substrate materials, and is uniquely suited to modelling magnetic information storage and processing where multi-physics and multi-material capabilities with flexible discretization are essential. A review of recent works using BORIS was also

given, discussing applications to hard-disk-drive reading and writing processes, namely by modelling magnetic read heads and digital bit writing in magnetic tracks, ultrafast magnetization dynamics processes, computation of thermodynamics equilibrium states using advanced Monte Carlo algorithms, as well as manipulation of skyrmions using electrical currents and focused laser beams. All computations may be performed on GPUs, both single and multiple GPUs, which establishes BORIS as one of the most powerful software for micromagnetic and atomistic spin systems modelling to date.

References

[1] S. Lepadatu, Boris computational spintronics — High performance multi-mesh magnetic and spin transport modelling software. J. Appl. Phys. 128, 243902 (2020). https://doi.org/10.1063/5.0024382
[2] T.L. Gilbert, A Lagrangian formulation of the gyromagnetic equation of the magnetic field. Phys. Rev. 100, 1243 (1955).
[3] D.A. Garanin, Fokker-Planck and Landau-Lifshitz-Bloch equations for classical ferromagnets. Phys. Rev. B 55, 3050 (1997). https://doi.org/10.1103/PhysRevB.55.3050
[4] D.A. Garanin and O. Chubykalo-Fesenko, Thermal fluctuations and longitudinal relaxation of single-domain magnetic particles at elevated temperatures. Phys. Rev. B 70, 212409 (2004). https://doi.org/10.1103/PhysRevB.70.212409
[5] R.F.L. Evans et al., Stochastic form of the Landau-Lifshitz-Bloch equation. Phys. Rev. B 85, 014433 (2012). https://doi.org/10.1103/PhysRevB.85.014433
[6] S. Zhang and Z. Li, Roles of Nonequilibrium Conduction Electrons on the Magnetization Dynamics of Ferromagnets. Phys. Rev. Lett. 93, 127204 (2004). https://doi.org/10.1103/PhysRevLett.93.127204
[7] S. Lepadatu, Effect of inter-layer spin diffusion on skyrmion motion in magnetic multilayers. Scientific Reports 9, 9592 (2019). https://doi.org/10.1038/s41598-019-46091-1
[8] C.R. MacKinnon, S. Lepadatu, T. Mercer, and P.R. Bissell "Role of an additional interfacial spin-transfer torque for current-driven skyrmion dynamics in chiral magnetic layers" Physical Review B 102, 214408 (2020). https://doi.org/10.1103/PhysRevB.102.214408
[9] M.I. Dyakonov and V.I. Perel, Possibility of orienting electron spins with current. JETP Lett. 13, 467-469 (1971).
[10] J.C. Slonczewski, Current-driven excitation of magnetic multilayers. J. Magn. Magn. Mater. 159, L1–L7 (1996). https://doi.org/10.1016/0304-8853(96)00062-5
[11] S. Lepadatu, Unifed treatment of spin torques using a coupled magnetisation dynamics and three-dimensional spin current solver. Scientific Reports 7, 12937 (2017). https://doi.org/10.1038/s41598-017-13181-x
[12] J.E. Hirsch, Spin Hall Effect. Phys. Rev. Lett. 83, 1834 (1999). https://doi.org/10.1103/PhysRevLett.83.1834
[13] Y. Tserkovnyak, A. Brataas, and G.E.W. Bauer, Enhanced Gilbert Damping in Thin Ferromagnetic Films. Phys. Rev. Lett. 88, 117601 (2002). https://doi.org/10.1103/PhysRevLett.88.117601
[14] Y. Tserkovnyak and M. Mecklenburg, Electron transport driven by nonequilibrium magnetic textures. Phys. Rev. B 77, 134407 (2008). https://doi.org/10.1103/PhysRevB.77.134407
[15] S. Zhang and S.S.-L. Zhang, Generalization of the Landau-Lifshitz-Gilbert Equation for Conducting Ferromagnets. Phys. Rev. Lett. 102, 086601 (2009). https://doi.org/10.1103/PhysRevLett.102.086601
[16] S. Lepadatu and A. Dobrynin, "Self-consistent computation of spin torques and magneto-resistance in tunnel junctions and magnetic read-heads with metallic pinhole defects" Journal of Physics: Condensed Matter 35, 115801 (2023). DOI 10.1088/1361-648X/acb2a6
[17] S. Lepadatu, Interaction of magnetization and heat dynamics for pulsed domain wall movement with Joule heating. J. Appl. Phys. 120, 163908 (2016). https://doi.org/10.1063/1.4966607
[18] U. Atxitia, and O. Chubykalo-Fesenko, Ultrafast magnetization dynamics rates within the Landau-Lifshitz-Bloch model. Phys. Rev. B 84, 144414 (2011). https://doi.org/10.1103/PhysRevB.84.144414
[19] S. Lepadatu, Efficient computation of demagnetizing fields for magnetic multilayers using multilayered convolution. J. Appl. Phys. 126, 103903 (2019). https://doi.org/10.1063/1.5116754
[20] I.A. Dzyaloshinsky, A thermodynamic theory of "weak" ferromagnetism of antiferromagnetics. J. Phys. Chem. Solids 4, 241-255 (1958).
[21] T. Moriya, Anisotropic superexchange interaction and weak ferromagnetism. Phys. Rev. 120, 91 (1960). https://doi.org/10.1103/PhysRev.120.91
[22] B. Heinrich et al., Bilinear and biquadratic exchange coupling in bcc Fe/Cu/Fe trilayers: Ferromagnetic-resonance and surface magneto-optical Kerr-effect studies. Phys. Rev. B 47, 5077 (1993). https://doi.org/10.1103/PhysRevB.47.5077
[23] S. Lepadatu, Effective field model of roughness in magnetic nano-structures. J. Appl. Phys. 118, 243908 (2015). https://doi.org/10.1063/1.4939093
[24] Source code repository: https://github.com/SerbanL/BORIS. Accessed on December 21st, 2023.
[25] J. Nickolls, I. Buck, M. Garland, and K. Skadron, Scalable Parallel Programming with CUDA. ACM Queue 6, 40-53 (2008). https://doi.org/10.1145/1365490.1365500
[26] S. Lepadatu, "Accelerating micromagnetic and atomistic simulations using multiple GPUs" J. Appl. Phys. 134, 163903 (2023). https://doi.org/10.1063/5.0172657
[27] E. Beaurepaire, J.-C. Merle, A. Daunois, and J.-Y. Bigot, Ultrafast spin dynamics in ferromagnetic nickel. Phys. Rev. Lett. 76, 4250 (1996). https://doi.org/10.1103/PhysRevLett.76.4250
[28] S. Lepadatu "Emergence of transient domain wall skyrmions after ultrafast demagnetization" Physical Review B 102, 094402 (2020). https://doi.org/10.1103/PhysRevB.102.094402
[29] R. Cheng, M. Li, A. Sapkota, A. Rai, A. Pokhrel, T. Mewes, C. Mewes, D. Xiao, M. De Graef, and V. Sokalski, Phys. Rev. B 99, 184412 (2019). https://doi.org/10.1103/PhysRevB.99.184412
[30] S. Lepadatu "Micromagnetic Monte Carlo method with variable magnetization length based on the Landau–Lifshitz–Bloch equation for computation of large-scale thermodynamic equilibrium states" Journal of Applied Physics 130, 163902 (2021). https://doi.org/10.1063/5.0059745
[31] S. Lepadatu, G. Mckenzie, T. Mercer, C.R. MacKinnon, P.R. Bissell, "Computation of magnetization, exchange stiffness, anisotropy, and susceptibilities in large-scale systems using GPU-accelerated atomistic parallel Monte Carlo algorithms" Journal of Magnetism and Magnetic Materials 540, 168460 (2021). https://doi.org/10.1016/j.jmmm.2021.168460
[32] K. Gerlinger, B. Pfau, F. Büttner, M. Schneider, L.-M. Kern, J. Fuchs, D. Engel, C.M. Günther, M. Huang, I. Lemesh et al., "Application concepts for ultrafast laser-induced skyrmion creation and annihilation" Appl. Phys. Lett. 118, 192403 (2021). https://doi.org/10.1063/5.0046033
[33] M.M. Vopson and S.Lepadatu, "Second law of information dynamics" AIP Advances 12, 075310 (2022). https://doi.org/10.1063/5.0100358
[34] S. Lepadatu, "All-Optical Magnetothermoelastic Skyrmion Motion" Physical Review Applied 19, 044036 (2023). https://doi.org/10.1103/PhysRevApplied.19.044036
[35] C.R. MacKinnon, K. Zeissler, S. Finizio, J. Raabe, C.H. Marrows, T. Mercer, P.R. Bissell, and S. Lepadatu, "Collective skyrmion motion under the influence of an additional interfacial spin-transfer torque" Scientific Reports 12, 10786 (2022). https://doi.org/10.1038/s41598-022-14969-2